Per. Mineral. (2000), *69*, 2, 185-204 http://go.to/permin

PERIODICO di MINERALOGIA
established in 1930

An International Journal of
MINERALOGY, CRYSTALLOGRAPHY, GEOCHEMISTRY, ORE DEPOSITS, PETROLOGY, VOLCANOLOGY
and applied topics on *Environment, Archaeometry* and *Cultural Heritage*

Distribution and representative whole-rock chemistry of deep-seated xenoliths from the Iblean Plateau, south-eastern Sicily, Italy

GIOVANNA SAPIENZA and VITTORIO SCRIBANO*

Dipartimento di Scienze Geologiche, Università di Catania, Corso Italia 55, I-95129 Catania (Italy)

Submitted, March 2000 - Accepted, May 2000

ABSTRACT. — Eighteen unpublished whole-rock chemical analyses on Iblean deep-seated xenoliths, combined with twenty-nine analyses reported in previous papers, form a data set representative of the various xenolith types as fixed by field and laboratory investigations lasting more than ten years.

All Iblean xenoliths can be split into two main groups: ultramafic (UL) and feldspar-bearing (FB). The former, mostly representing the lithospheric mantle, consists of peridotites (UL-a) and various pyroxenites (UL-b-c-d). The peridotites exhibit a moderately refractory character, with some enrichment in LREE and other incompatible elements due to metasomatic event(s). The pyroxenites (spinel-websterites in most cases) derive from crystallisation and later sub-solidus re-equilibration of basic melts intruding the peridotites at different mantle depths. We distinguish Cr-rich and Al-poor pyroxenites (group UL-b, green) from those Cr-poor and Al-rich (groups UL-c, UL-d, black). Only the latter group keep their original igneous texture, but minor sub-solidus transformations occur. Garnet is found in some Al-rich pyroxenites, especially in those of group UL-d. The garnet, where modally abundant, controls the whole-rock distribution of some trace elements, especially REE.

Fully recrystallized two-pyroxene granulites are the most common feldspar-bearing lithotypes (FB-e) together with minor cumulitic gabbros (group FB-f), variously recrystallized anorthosites (FB-g), rare metadiorites (FB-h) and plagioclase-websterites (FB-i). The representative whole-rock chemical compositions confirm such a division on a petrographic basis for most of the FB xenoliths.

The chemical data set considered here, coupled with estimates of relative abundances of the various xenolith groups, may suggest the Iblean upper-mantle and inaccessible crust bulk compositions. The first exhibits a Primordial Mantle composition, due to the refertilizing effect of pyroxenites on the barren peridotites. Instead, the crust shows a roughly basaltic composition. Assuming that the Iblean xenoliths adequately represent all parts of the lithospheric column, which is probable for diatreme-related xenoliths, there is a marked absence of any felsitic upper crustal lithology. This fact may depend on (1) extreme lamination of a previous continental crust by rifting processes and concomitant magmatic intrusions and underplating, (2) severe erosion of the upper continental crust during an (unknown) period of exhumation, (3) the oceanic nature of the Iblean lithosphere.

RIASSUNTO. — Alle 29 analisi chimiche in toto di xenoliti degli Iblei presentate in varie pubblicazioni

* Corresponding author, E-mail: scribano@mbox.unict.it

si aggiungono 18 nuove analisi, al fine di ottenere un insieme di dati più rappresentativo delle diverse litologie riconosciute in molti anni di indagini sul terreno e in laboratorio. Tutti gli xenoliti sono stati suddivisi in base alla presenza o meno di feldspato. Gli ultrafemici (UL), per lo più riferibili al mantello litosferico, sono costituiti da peridotiti (UL-a) e diverse pirosseniti (UL-b-c-d). Le prime presentano un carattere moderatamente refrattario ove tuttavia l'arricchimento in alcuni elementi incompatibili (es. LREE) è ascrivibile ad eventi metasomatici. Le pirosseniti (per lo più websteriti a spinello) derivano dalla cristallizzazione di diversi liquidi basici intrusi nelle peridotiti a varie profondità ove talora hanno subito profonde modificazioni a temperature sub-solidus, come suggerito dai loro caratteri composizionali e tessiturali. Sono presenti pirosseniti ricche in Cr e povere in Al (gruppo UL-b, di colore verde) e viceversa (gruppi UL-c e UL-d, di colore nero). Tra queste ultime soltanto le UL-d conservano l'originaria struttura ignea. In alcune pirosseniti ricche in alluminio, sopratutto del gruppo UL-d, è talora presente il granato che, in qualche caso, condiziona pesantemente la distribuzione di alcuni elementi in tracce, in particolare le terre rare, nella roccia in toto.

I noduli a feldspato sono granuliti basiche a due pirosseni e Al-spinello (gruppo FB-e), gabbri cumulitici (FB-f), anortositi (FB-g), rare metadioriti (FB-h) e websteriti a plagioclasio (FB-i). I dati chimici confermano tale classificazione petrografica, sebbene le anortositi e le websteriti potrebbero essere anche considerate opposti estremi del gruppo delle granuliti. Anche queste rocce, tutte riferibili a livelli crostali presumibilmente profondi, presentano una più o meno lontana origine da magmi basici.

I dati analitici a disposizione sono sufficientemente rappresentativi delle varietà litologiche degli xenoliti iblei. Per tale motivo sono state stimate le rispettive percentuali in volume e si è proceduto al calcolo delle medie pesate delle composizioni degli xenoliti ultrafemici (mantellici) e di quelli a feldspato (crostali). I primi, nell'insieme, mostrano una composizione piuttosto simile a quella del Mantello Primordiale. I secondi, invece, hanno una composizione di tipo grosso modo basaltico.

Gli xenoliti rappresentano adeguatamente tutta la colonna litosferica (il che è verosimile per gli xenoliti presenti nei diatremi, come accade in varie località. L'assenza di litotipi felsitici (l.s.) ascrivibili alla parte alta della crosta continentale può derivare da un'estremo assottigliamento in seguito a episodi di rifting e concomitanti copiose intrusioni di masse magmatiche basiche o da una profonda erosione durante un ipotetico periodo di esposizione a giorno, oppure la litosfera sub-iblea presenta un'affinità oceanica.

KEY WORDS: *Sicily, xenoliths, lithosphere, geochemistry, petrology.*

INTRODUCTION

The Iblean Plateau (south-eastern Sicily, Italy) consists of a Mesozoic-Cenozoic carbonate sequence and Neogene-Quaternary clastics with several intercalations of basic volcanic rocks. Since the beginning of the Neogene, the Iblean area has represented the foreland of south-verging nappes related to the collisional movements of the African and European plates (Longaretti and Rocchi, 1990). Fissural eruptions, both submarine and subaerial, occurred in the northern sector of the Plateau along a NW-SE wrench fault system. The magmatic products related to the Iblean Neogene-Quaternary eruptive activity consist of tholeiitic basalts, alkaline basalts and minor basanites, nephelinites, hawaiites and tephrites (Beccaluva *et al.*, 1998; Trua *et al.*, 1998).

Deep-seated xenoliths were found in some diatreme-related tuff-breccia deposits of Upper Miocenic age and in some Quaternary basanitic and nephelinitic lava flows (Scribano, 1987a, 1987b). The diatremes are of prime importance, since their relatively low eruptive temperatures and the high ascending velocity of the eruptive column through the vent may preserve the xenoliths from severe reaction with the host magma (e.g. Ferrini and Sassano, 1999, and references therein). In addition, xenoliths occurring in world-wide *diatremes* usually represent most parts of the lithospheric column (e.g. Hawthorne, 1975; Dawson, 1980). Carbone and Lentini (1981) mention several Miocenic diatremes in the Iblean area: nevertheless, relatively abundant xenoliths were found only in the Cozzo Molino pipe (site «1» in fig. 1) and the tuff-breccia deposits in Valle Guffari (site «2» in fig. 1). The latter represents the most significant xenolith occurrence in the Iblean Region (and, probably,

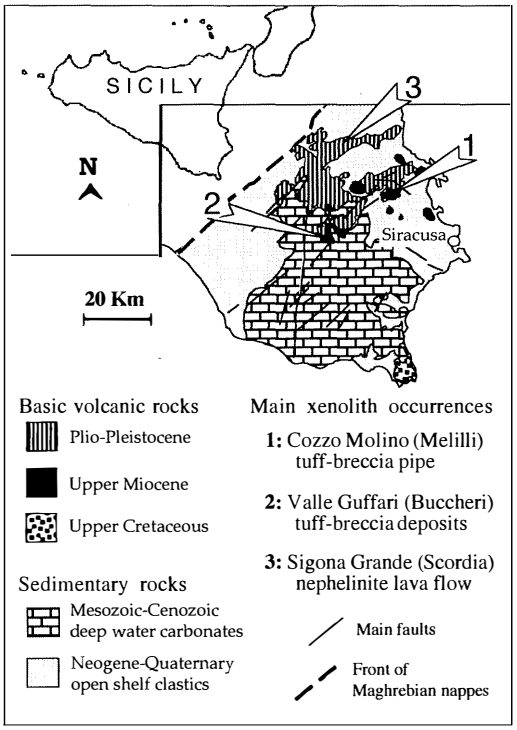

Fig. 1 – Location of main xenolith occurrences.

in the Central Mediterranean area). It consists of lapilli-sized clasts of basanitoid juvenile lava and inequigranular lithics, with a fine palagonitic matrix and minor carbonatic and zeolitic cement. The xenoliths appear irregularly distributed within the host breccia, with some striking concentrations probably related to flow differentiation mechanisms. They exhibit variously rounded, discoidal or elongated shapes. Large samples (up to 30 cm in length, more than 1 kg in weight) are not rare, although the most common size is 3.5 cm: e.g. Punturo and Scribano (1997).

Some Quaternary basanite and nephelinite lavas cropping out along the northern margin of the Iblean Plateau bear deep-seated xenoliths. Worth noting is a melanocratic nephelinite lava at Sigona Grande (site «3» in fig. 1) because of the great quantity of xenoliths. They exhibit various angular or rounded shapes, and vary from less than 1 cm up to 5 cm, 2 cm being the average size.

Essential petrographic features and distribution of Iblean xenoliths

Iblean xenoliths may be split into two main groups on the basis of their mineralogical modal composition: ultramafic (UL) and feldspar-bearing (FB). A number of pressure-temperature estimates suggests that in most cases the first group represents mantle xenoliths and the second group inaccessible crust xenoliths (e.g. Nimis, 1998; Tonarini *et al.*, 1996; Atzori *et al.*, 1999, and unpublished data). Further textural and mineralogical features allow these two xenolith groups to be divided into nine additional sub-groups: four for the ultramafic UL-(a,b,c,d) and five for the feldspar-bearing types FB-(e,f,g,h,i). The following petrographic description derives from previous papers (Scribano, 1986, 1987a, 1987b, 1988a, 1988b, 1995; Punturo, 1997; Tonarini *et al.* 1996; Atzori *et al.*, 1999) and unpublished data.

Ultramafic xenoliths

Spinel-peridotites (olivine, Ca-poor pyroxene, spinel, calcic pyroxene) form the UL-a group. Those occurring in the Miocene tuff-breccia deposits consist of spinel-lherzolites and harzburgites with protogranular texture: coarse (up to 5 mm) kink-banded olivine and smaller pyroxene grains show curvilinear grain boundaries. Cr-Al-spinel occurs either as interstitial grains or as vermiform intergrowths with the clinopyroxene. This shows a «dusty» aspect due to a number of tiny inclusions of CO_2, spinel, glass and ores. We should also note the rare occurrence of texturally equilibrated phlogopite, primary carbonate and veinlets of silicate glass. Local modal increasing in orthopyroxene or clinopyroxene often form irregular, generally elongated, olivine-

pyroxenite patches in our peridotites. In addition, cm-size websterite veins, with planar contacts, give some nodules a striking composite character. Such pyroxenite enrichments and veins are well documented in world-wide xenoliths and Alpine-type peridotites, being generally interpreted as the result of various metamorphic and igneous processes within the upper mantle (e.g. Morten and Obata, 1983). Peridotite xenoliths from the Quaternary lavas exhibit textures intermediate between protogranular and porphyroclastic (very common), porphyroclastic (common) and equigranular-mosaic (rare). Except for texture, all other petrographic and mineralogical aspects are similar to the peridotites from Miocene diatremes. It must be noted that even the freshest Iblean peridotites exhibit some serpentine content.

The other three groups of ultramafic xenoliths (UL-b, UL-c, UL-d) consist of various pyroxenite types. We ascribe to group UL-b spinel-websterites, showing green colour (from pale to very dark green) due to the presence of a green chromian diopside, together with orthopyroxene, Al-Cr-spinel, ores, rare olivine and very rare chromian pargasite replacing the clinopyroxene. Their texture is xenomorphic granular in most cases. Greyish-green orthopyroxene-rich websterites also belong to this group. The most significant UL-b group websterites form veins and irregular pockets within some peridotites, hence occurring as composite xenoliths.

Dull-black, fully recrystallized websterites constitute group UL-c. They consist of clino- and ortho-pyroxenes and Al-spinel showing triple point junctions. Rare sub-solidus garnet occurs between spinel and pyroxene. Calcic pyroxene grains appear larger and are usually more abundant than the other co-existing minerals. Both calcic and Ca-poor pyroxene display evident exsolution features.

Clinopyroxenites with an Al-rich ($8 \leq Al_2O_3$wt% ≤ 11), low-Ca (CaO = 17wt% ca.) clinopyroxene, abundant aluminous spinel and/or garnet and minor orthopyroxene form group UL-d. In most cases, these rocks show evident poikilitic texture (except minor recrystallized zones) with very coarse (up to 8 cm in length) clinopyroxene oikocrysts enclosing euhedral spinel grains. The clinopyroxene is compositionally homogeneous, although it exhibits wide «spongy» zones, due to the occurrence of a number of droplets of partial melting glass. In some cases, the extent of partial melting is so great that it obliterates both the cumulate texture and the megacrystic grain size. The modal abundance of spinel is antithetic with garnet. The textural features of the latter do not unambiguously suggest its magmatic or sub-solidus origin: large patches of anhedral garnet (widely transformed into kelyphite) enclose rounded clinopyroxene and rare spinel grains, which show reaction coronas. In rarer cases, spinel is absent and coarse euhedral garnet grains suggest a probable cumulus origin. Because of the petrologic importance of garnet, we further distinguish garnet-bearing (UL-d′) from garnet-free samples (UL-d). We also associate with group UL-d some megacryst «discrete nodules» of clinopyroxene similar to that of the cumulates above, which thus represent fragments of original polycrystalline rocks.

Feldspar-bearing xenoliths

Feldspar-bearing xenoliths (group FB) are relatively abundant and very well preserved in the Miocene tuff-breccia deposits. They are considered to be of crustal origin. The mantle / crust xenolith ratio (volume) is about 70:30. Conversely, in the Quaternary lavas crustal xenoliths are very rare (no more than 2% in volume with respect to ultramafic xenoliths) and strongly reabsorbed by the host lavas. Their modal compositions, mineral chemistry and texture suggest an igneous origin (with basic and intermediate compositions in most cases), despite their various and complex sub-solidus histories. Basic granulites, with plagioclase (An_{45-70}), coexisting calcic and Ca-poor pyroxenes and Al-spinel, are the most common lithotypes (FB-e) in the feldspar-bearing group. They exhibit annealed texture

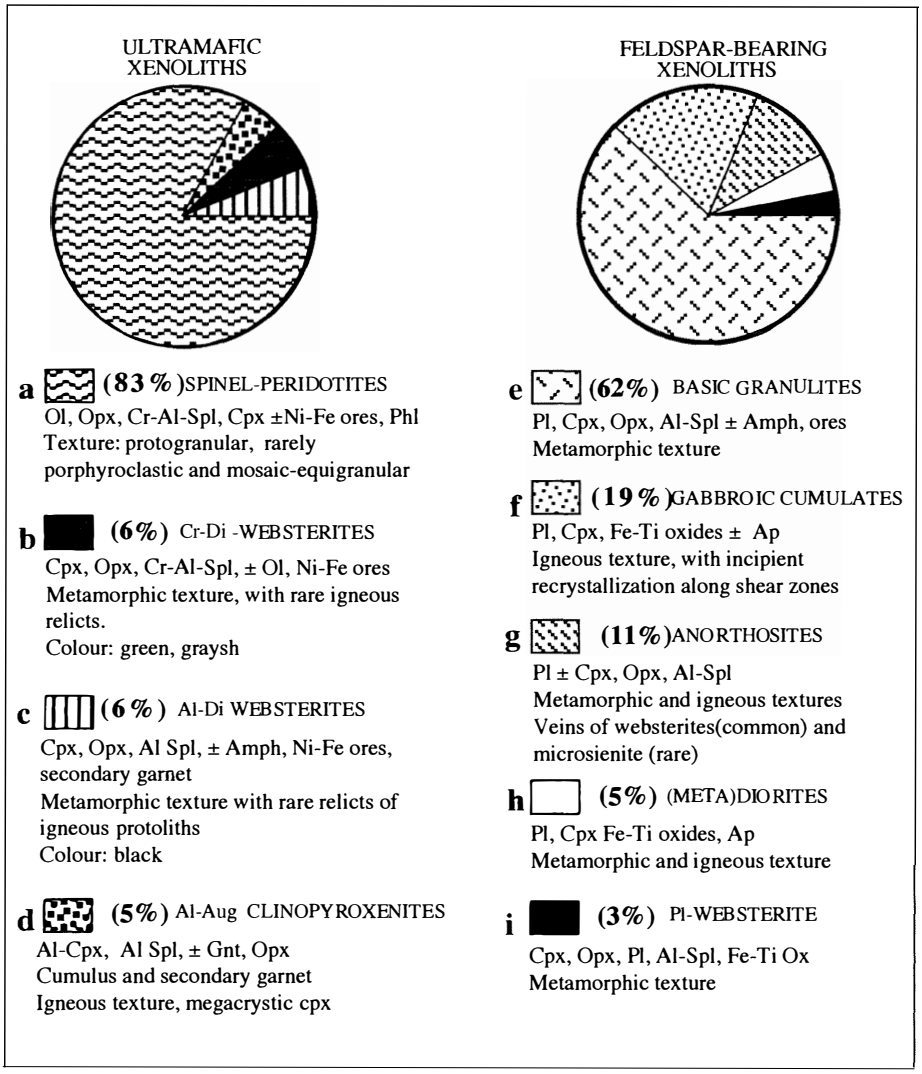

Fig. 2 – Distribution (by percentage volume) of different types of Iblean deep-seated xenoliths (mineral symbols after Kretz, 1983).

with differing grain sizes, mineral chemistry and modal proportions of their constituent minerals. Indistinct gneissoic banding is a common feature of these rocks, as well as various disequilibrium textures. Very rarely pargasitic amphibole replaces the pyroxene. Instead, some gabbroic xenoliths (group FB-f) show evident cumulate texture, except for minor zones of neoblastic subgrains associated with complex deformation features. These gabbros consist of elongated plagioclase and shillerized clinopyroxene grains, Ti-magnetite, apatite, and rare sub-solidus Al-spinel.

Variously recrystallized anorthosite xenoliths are ascribed to group FB-g. They sometimes show veins of spinel-websterites and, more

TABLE 1

Whole-rock chemical analyses of some representative ultramafic (UL) and feldspar-bearing (FB) xenoliths from Iblean area. Petrographic sub-groups (a, b, c etc.) shown in fig. 2.

wt%	UL-a23	UL-a8	UL-a77	UL-b3	UL-b36	UL-c25	UL-c48	UL-d2	UL-d4	UL-d21	UL-d46	UL-d47	FB-f1	FB-f31	FB-f4	FB-f7	FB-h2	FB-h3
SiO_2	42.0	43.3	41.9	50.4	49.2	48.1	43.0	41.5	40.1	48.1	42.2	43.9	36.4	38.9	42.3	45.4	57.2	51.2
TiO_2	0.0	0.1	0.0	0.2	0.8	0.9	1.1	1.1	1.2	0.9	0.9	1.2	5.4	5.5	3.1	1.9	0.2	2.1
Al_2O_3	1.2	2.0	1.9	3.9	7.2	9.1	8.2	16.0	15.9	8.4	15.4	14.6	10.0	15.2	16.7	19.2	22.3	17.4
Fe_2O_3	8.5	8.7	8.8	6.7	7.6	7.7	10.6	9.5	9.4	11.0	8.9	10.4	22.3	15.9	11.2	9.6	1.5	5.6
MnO	0.1	0.1	0.1	0.1	0.1	0.1	0.1	0.1	0.1	0.2	0.1	0.2	0.2	0.1	0.1	0.1	0.0	0.1
MgO	39.3	36.9	36.8	26.7	17.3	15.5	18.0	15.4	14.0	15.7	15.5	14.2	9.0	6.4	7.1	5.1	1.9	2.2
CaO	3.2	4.1	3.9	9.2	15.3	15.7	13.7	14.5	15.0	13.8	14.9	12.5	13.4	12.7	14.8	11.4	5.7	8.8
Na_2O	0.1	0.0	0.0	0.3	1.0	1.1	0.8	1.0	0.7	1.1	1.0	1.1	1.3	1.8	1.4	3.0	7.3	6.3
K_2O	0.0	0.0	0.0	0.0	0.0	0.1	0.0	0.0	0.0	0.0	0.0	0.1	0.1	0.3	0.1	0.4	0.6	1.4
P_2O_5	0.1	0.1	0.1	0.1	0.1	0.1	0.1	0.1	0.1	0.0	0.0	0.2	0.1	0.3	0.2	0.1	0.1	0.6
H_2O	4.3	3.7	5.2	1.7	0.9	1.4	3.4	0.7	3.2	0.9	0.7	1.9	0.9	2.4	2.9	3.2	3.0	0.8
CO_2	1.6	1.4	1.7	0.3	0.6	0.1	1.5	0.1	0.3	0.1	0.3	0.1	0.1	0.2	0.1	0.3	0.3	3.6
tot	100.3	100.4	100.5	99.6	99.9	99.9	100.0	100.0	100.4	100.4	100.0	99.9	99.0	99.9	100.1	99.6	100.2	99.8
ppm																		
La	1.3	2.9	1.3	4.9	3.2	2.4	3.7	3.2	3.8	0.8	1.8	4.4	4.5	5.9	5.9	6.8	5.5	31.7
Ce	2.6	4.5	2.1	9.6	8.2	6.9	10.6	9.3	9.0	3.1	6.7	10.8	17.5	14.5	14.5	14.6	9.2	67.9
Pr	0.3	0.4	0.2	1.0	1.2	1.2	1.7	1.5	1.4	0.6	1.2	1.6	3.2	2.1	2.2	2.1	1.0	9.0
Nd	1.2	1.5	0.8	3.5	6.6	6.1	10.0	8.2	7.7	3.9	7.2	8.2	19.4	10.5	11.2	9.8	4.0	40.0
Sm	0.3	0.2	0.1	0.7	2.0	2.3	2.8	2.6	2.9	1.8	2.2	2.6	5.2	2.9	2.9	2.2	0.7	7.6
Eu	0.1	0.1	0.0	0.3	0.7	0.8	1.0	1.0	1.0	0.6	0.9	1.1	2.0	1.3	1.3	1.6	1.1	4.9
Gd	0.2	0.3	0.1	0.8	2.1	2.7	2.7	3.2	3.1	2.5	2.7	3.3	5.9	2.9	3.0	2.3	0.6	6.5
Tb	0.0	0.0	0.0	0.1	0.3	0.4	0.4	0.4	0.5	0.4	0.4	0.6	0.8	0.4	0.4	0.3	0.1	0.8
Dy	0.2	0.2	0.1	0.8	2.0	2.3	2.3	2.5	2.5	2.5	2.6	4.8	4.1	2.1	2.1	1.6	0.4	4.0
Ho	0.0	0.1	0.0	0.2	0.4	0.5	0.4	0.5	0.5	0.5	0.5	1.1	0.8	0.4	0.4	0.3	0.1	0.7
Er	0.1	0.2	0.1	0.4	0.9	1.3	1.1	1.2	1.1	1.2	1.3	3.0	1.9	0.9	0.8	0.7	0.2	1.7
Tm	0.0	0.0	0.0	0.1	0.1	0.2	0.1	0.2	0.2	0.2	0.2	0.5	0.3	0.1	0.1	0.1	0.0	0.2
Yb	0.1	0.1	0.1	0.3	0.7	1.0	0.8	1.0	0.9	1.0	1.1	3.7	1.4	0.7	0.7	0.5	0.2	1.1
Lu	0.0	0.0	0.0	0.1	0.1	0.2	0.1	0.2	0.1	0.2	0.2	0.6	0.2	0.1	0.1	0.1	0.0	0.2
$(La/Sm)_n$	2.9	8.8	7.5	4.3	1.0	0.7	0.8	0.8	0.8	0.3	0.5	1.1	0.5	1.3	1.2	1.9	4.7	2.6
$(La/Yb)_n$	11.4	16.7	9.0	9.9	2.9	1.5	3.2	2.1	2.9	0.5	1.1	0.8	2.2	6.1	5.7	8.8	24.8	18.9
V	56.2	73.8	75.6	152.6	328.1	337.5	413.9	221.5	291.3	231.2	281.2	283.1	534.8	10.8	99.6	439.7	310.3	261.2
Cr	2618.1	3207.6	2867.2	4693.4	61.4	154.5	62.8	1530.4	35.2	803.1	1139.7	270.4	56.8	2.5	7.6	11.4	119.0	55.8
Co	107.4	108.8	113.2	65.2	71.6	77.0	88.4	47.5	65.5	96.8	61.1	47.2	61.8	3.7	8.8	59.2	36.4	34.9
Ni	2002.8	1991.9	2046.0	1146.7	465.1	379.9	399.7	427.4	285.8	359.8	454.2	307.7	60.3	12.2	23.6	34.1	82.9	71.2
Cu	5.1	31.7	14.1	127.1	80.6	46.7	44.6	48.8	102.0	15.4	168.1	56.9	49.3	7.9	25.3	37.9	64.1	43.7
Zn	51.8	55.9	53.0	39.3	132.2	156.8	242.1	49.6	73.8	93.5	77.0	62.3	219.3	11.6	57.8	112.9	101.6	85.8
Sr	196.3	81.5	194.9	142.6	89.0	403.8	150.2	65.6	530.7	29.5	55.2	564.6	1063.6	2276.2	2736.1	3457.7	1135.0	859.8
Rb	0.6	0.5	0.6	0.4	1.7	4.6	1.0	0.6	3.4	0.6	0.7	5.0	3.3	16.0	5.8	16.3	14.3	9.2
Ba	3.0	1.9	1.5	2.6	17.2	138.7	3.2	15.8	167.4	0.6	4.4	952.1	83.9	605.1	143.1	469.8	483.7	2480.0
Th	0.1	0.3	0.1	0.5	0.2	0.1	0.2	0.2	0.2	0.0	0.0	0.2	0.0	0.3	0.1	0.1	0.1	0.3
Ta	0.1	0.1	0.0	0.0	0.2	0.1	0.2	0.2	0.1	0.0	0.1	0.2	0.7	0.6	0.4	0.3	0.1	1.6
Nb	0.9	1.5	0.7	1.5	2.6	1.3	2.1	1.7	1.4	0.4	0.7	2.6	7.1	7.0	4.6	2.9	1.4	24.0
Zr	3.2	6.0	2.0	5.3	28.0	28.5	39.3	35.9	39.3	22.6	29.4	45.7	59.8	39.8	41.3	22.7	9.9	21.5
Hf	0.1	0.2	0.0	0.2	1.0	1.2	1.5	1.4	1.7	1.1	1.3	1.3	2.1	1.1	1.3	0.7	0.2	0.5
Y	0.7	1.2	0.6	3.9	10.7	12.8	11.7	13.9	13.1	13.6	13.2	34.2	20.6	10.5	10.8	8.1	2.1	18.7

rarely, veins of a quartz-free microsienite (composite xenoliths). The latter is the most potassic rock ever found in the Iblean Region. In both cases, the veins were fully equilibrated with the host anorthosite at sub-solidus temperatures. Rare xenoliths with roughly dioritic composition form group FB-h. Their texture consists of a mass of poorly twinned, irregularly interlocked plagioclase grains showing striking undulose extinction, alternating with discontinuous layers of pyroxene grains. The latter are widely replaced by an optically unresolvable, yellowish aggregate of phyllosilicates and abundant calcite micrograins. Also note the absence of aluminous spinel and the relatively sodic character of the plagioclase (An_{30-45}). Some of these xenoliths have brittle fractures filled with veins of a strongly transformed silicate glass. We ascribe to the same group FB-h rare, strongly deformed plagioclase (An_{30}) megacryst (up to 25 cm in length) «discrete nodules». The last group of the feldspar-bearing xenoliths consists of rare orthopyroxene-rich, websterites (FB-i) bearing about 10% (by volume) modal plagioclase (An_{85-90}).

The distribution estimates of fig. 2 are based on more than 1000 xenoliths recognised in the field, 200 observed under the optical microscope, and about 100 analysed for mineral chemistry by EMPA. Nevertheless, the above-suggested distribution is only roughly indicative because of inevitable errors during field identification and counting of xenoliths. Only xenoliths larger than 15 cm and very representative of the nine (sub)groups were chosen for whole-rock chemical analyses.

WHOLE-ROCK CHEMISTRY OF THE IBLEAN XENOLITHS

Up to the present, there are 29 published whole-rock analyses of Iblean xenoliths (Mazzoleni and Scribano, 1994; Tonarini *et al.*, 1996; Punturo and Scribano, 1997). We add to these 18 new analyses (Table 1) in order to obtain a data set more representative of all the above-mentioned petrographic groups and sub-groups. The number of analysed samples from a given group is related to the importance of that group with respect to the whole xenolith mass and also depends on both the extent of the petrographic variations occurring within that group. These new analyses were performed at the SARM Laboratory (Nancy, France) by ICP (major elements) and ICP-MS (trace elements). Iron is reported as total divalent (FeO*) and the mg* number is calculated as MgO /(MgO + FeO*) molar ratios. Element detection limits and further detailed information on the analytical methods are reported in the SARM web site *http://www.crpg.cnrs-nancy.fr.*

MANTLE XENOLITHS

Major elements

Most of the examined ultramafic xenoliths exhibit different Al_2O_3 contents (from 0.86% up to 15.95%). Hence, alumina-based variations may represent a useful chemical discriminating factor (fig. 3).

Peridotite major element distributions (high MgO, relatively low SiO_2, Al_2O_3, CaO, TiO_2 etc.) conform to their elevated abundances of modal Mg-olivine. In more detail, two peridotite specimens have CaO contents (5.17-8.83%) higher than the other five (0.69-2.57%), in accordance with the prevalence of harzburgites over lherzolites among the Iblean peridotite xenoliths. Nevertheless, the lherzolitic nature of some xenoliths is not always a primary feature, due to the above mentioned zonal pyroxene enrichments.

Alumina and silica variations in pyroxenite xenoliths show evident inverse correlation (fig. 3). This fact depends on the modal ratio of Al-spinel and pyroxenes in these rocks. Pyroxenites representative of group UL-d show the highest Al_2O_3 (15-17%) and lowest SiO_2 (40-45%) (with the exception of one garnet-bearing, spinel-free clinopyroxenite, UL-d21 (fig. 3). Websterites from group UL-b lie at the opposite extremity of the trend and those from group UL-c are distributed centrally (fig. 3).

TABLE 2

Calculated chemical composition averaging 33 ultramafic xenoliths (UL.AV.) and 13 feldspar-bearing xenoliths (FB.AV.) on basis of percentage volume estimates, as in fig. 2.

	UL.AV.	FB.AV.
wt%		
SiO_2	47.28	49.33
TiO_2	0.07	1.12
Al_2O_3	1.45	20.43
FeO*	8.90	6.19
MnO	0.14	0.09
MgO	39.19	7.16
CaO	2.82	12.96
Na_2O	0.07	2.47
K_2O	0.03	0.16
P_2O_5	0.05	0.09
ppm		
La	2.27	3.12
Ce	4.93	7.44
Nd	2.32	5.11
Sm	0.57	1.30
Eu	0.20	0.74
Tb	0.10	0.20
Yb	0.28	0.44
Lu	0.04	0.07
V	89.00	156.89
Cr	2401.30	291.99
Co	106.80	34.63
Ni	1700.45	142.76
Zr	10.16	17.87
Y	2.86	5.26
Ba	32.67	159.24

The generally elevated CaO contents shown by all the examined pyroxenites reflect the common dominance of calcic over Ca-poor pyroxenes, except for some orthopyroxene-rich UL-b websterites (identified as b′ in fig. 3). High Cr, MgO, SiO_2 and low Al_2O_3 and TiO_2 abundances represent the most distinctive chemical features of UL-b pyroxenites (fig. 3). Alumina contents in websterites from the UL-c group show generally positive correlations with TiO_2 and FeO and negative correlation with Cr, except for sample UL-d21. Rocks from group UL-d do not show such correlations, but are characterised by very low contents of chromium (fig. 3).

Bivariate ratio plots of mg* *vs* SiO_2/Al_2O_3 (fig. 4) show that most UL-d pyroxenites plot in a restricted field, near that of primitive basaltic liquids (Kempton *et al.*, 1995). Notably, the UL-d positions, relative to the basaltic liquids field, may depend on the accumulation of Al-spinel and some removal of Fe-oxides. But sample UL-d21 is far from the above samples, because of its higher silica/alumina ratio. This fact may be ascribed to the minor amount of modal garnet, since the pyroxenes exhibit somewhat similar composition for all UL-d rocks (Punturo and Scribano, 1997, Sapienza and Scribano, unpublished). In the same diagram, UL-c websterites plot along a trend which may indicate pyroxene accumulation.

In summary, the distribution of most major elements in the examined ultramafic xenoliths appears roughly consistent with the proposed division into four petrographic sub-groups.

Chondrite normalized REE distribution

Iblean peridotite xenoliths (UL-a) show roughly chondritic abundances of MREE (1-0.08 × chondrite), slight HREE depletion and some LREE enrichment (5-10 × chondrite; La_n/Yb_n=3.85–21.48 and La_n/Sm_n =1.86-8.73). Moreover, all the analysed samples exhibit coherent patterns (fig. 5). Conversely, pyroxenites show various REE patterns, not always consistent with the above grouping on a petrographic basis. Websterites from group UL-b exhibit REE patterns close to those of peridotites (La_n/Sm_n=1-4.34; La_n/Yb_n=2.11-9.92), except for two samples showing a quite flat chondritic pattern from La to Eu at 10 × C1 and a slight depletion of HREE (fig. 5).

Most of the UL-c and UL-d pyroxenites show more or less pronounced upward-convex REE patterns, with several exceptions: some samples show variable enrichments in LREE (25-35 × chondrite; La_n/Sm_n=1.49-2.34 and

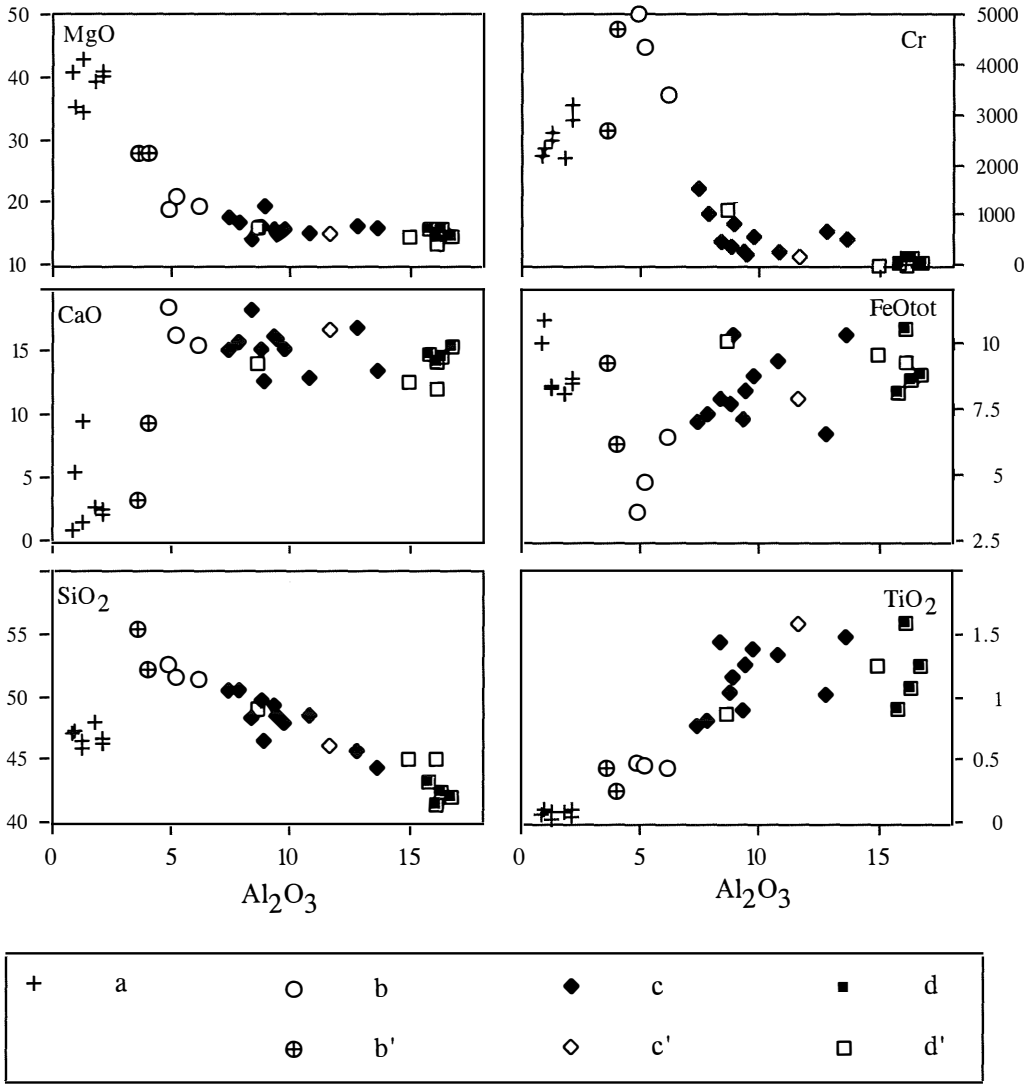

Fig. 3 – Major element and Cr variation diagrams of Iblean UL xenoliths as a function of Al_2O_3. Petrographic sub-groups as in fig. 2.

La_n/Yb_n=4.2-4.97) and one UL-d garnet-pyroxenite (UL-b47) exhibits significant HREE enrichment (Yb_n=17.57 × chondrite) (fig. 5).

The sum of REE in the examined peridotites (UL-a) is directly correlated to their CaO contents, which mostly depend on modal abundance of clinopyroxene (fig. 6): since the Iblean peridotite clinopyroxenes always show a number of diverse microinclusions, we hypothesize that such inclusions may be responsible for whole-rock LREE enrichment. Note that LREE enrichment in otherwise depleted peridotites is a common feature in world-wide mantle xenoliths. Many authors

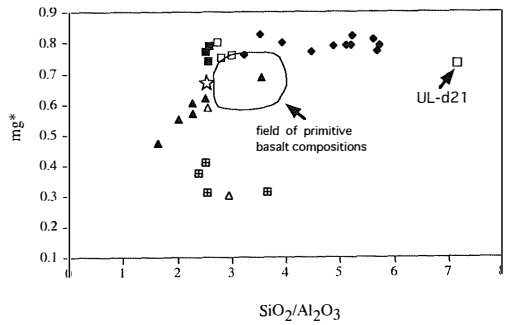

Fig. 4 – SiO_2/Al_2O_3 *vs* mg* of some UL and FB Iblean xenoliths. Field for primitive basaltic compositions following Kempton et al., 1995. Petrographic sub-groups as in fig. 2. Symbols as in figs. 3 and 10, star: averaged crustal Iblean xenolith compositions; full explanation in text.

ascribe such an enrichment to some deep-seated metasomatic agent or «b-component» (Frey and Prinz, 1978). The REE patterns in the Cr-rich, UL-b pyroxenites conform those of peridotites. (see above): probably, complete re-equilibration of these pyroxenites with the host peridotite led to a similar REE distribution (Frey and Prinz, 1978). Instead, the upward-convex REE pattern shown by most UL-c and UL-d pyroxenites suggests their cumulate origin (Frey and Prinz, 1978; Frey, 1980; Hart and Dunn, 1993).

One garnet clinopyroxenite (UL-b21) is remarkable for its relatively strong LREE depletion (La_n/Yb_n=0.5), close to one spinel-olivine-clinopyroxenite xenolith (PA-45) from

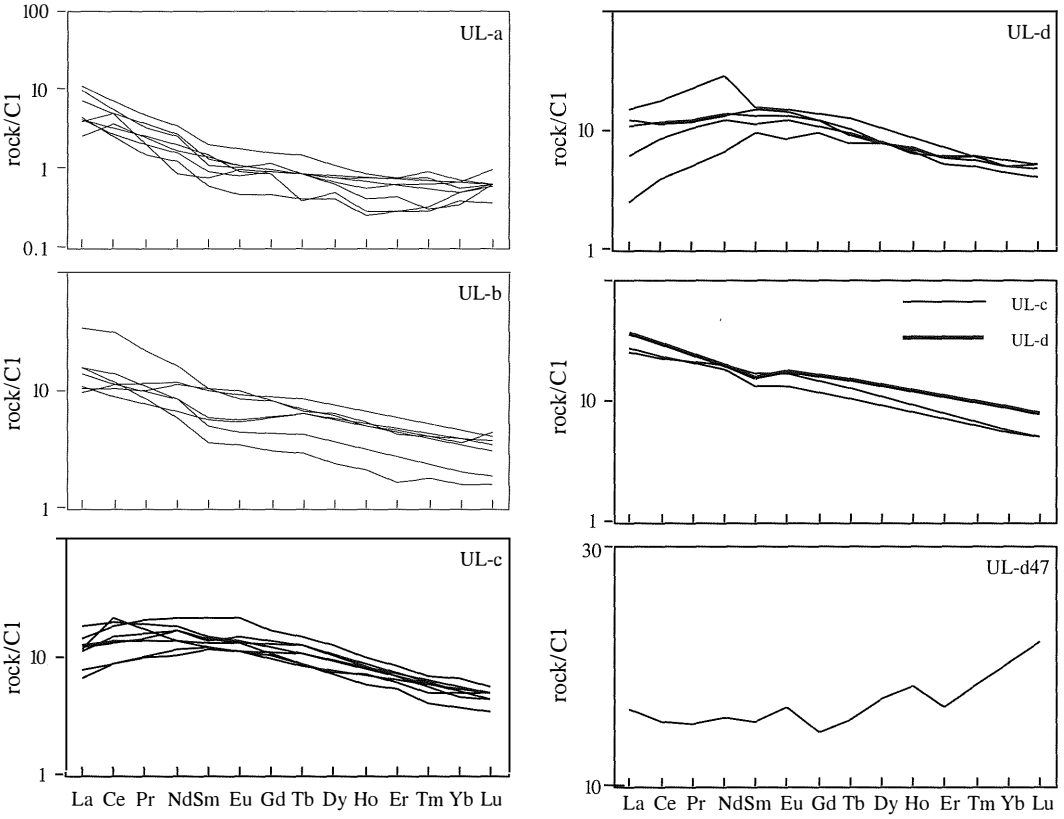

Fig. 5 – C1-normalized REE patterns of UL xenoliths (normalizing values of Boynton, 1984). Petrographic sub-groups as in fig. 2.

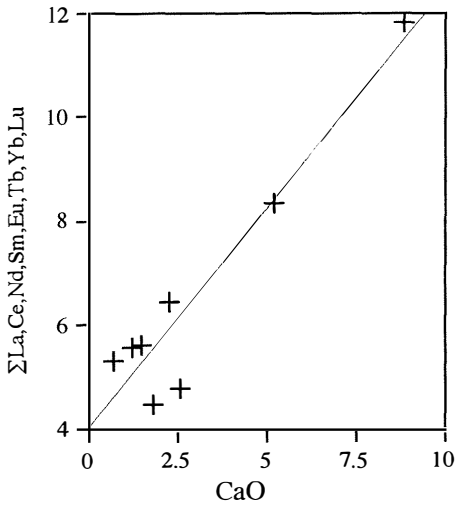

Fig. 6 – CaO *vs* sum of (La, Ce, Nd, Sm, Eu, Tb, Yb, Lu) of Iblean peridotites (crosses); *r:* linear correlation curve (y=4+0.86x).

San Carlos (Arizona) reported by Frey and Prinz (1978), who suggest the tholeiitic nature of the calculated equilibrium liquids for this rock. Lastly, the REE pattern shown by the UL-d47 pyroxenite conforms to the elevated modal content of garnet in this rock (about 30% by volume) following the compilation of REE garnet/basic-melt partition coefficients reported by Rollinson (1993).

Primordial-mantle normalized multi-element diagrams

Peridotites (UL-a) exhibit patterns moderately oscillating around primordial mantle (PM) abundances for LILE, with a linear, somewhat negative slope for the HFSE and a positive anomaly for P (fig. 7). UL-b websterites also roughly conform to PM abundances, except two samples showing slight Sr and significant Ba (20 × PM) enrichment. UL-c pyroxenites exhibit wide, mostly concordant, variations for LILE with evident enrichments of Sr and Ba (up to 50 × PM). Instead, the HFSE show flat, coherent trends at about 8 × PM. The UL-d pyroxenites copy the previous distribution but show more pronounced variations for the LILE (e.g. Ba varies from 0.1 × PM up to 100 × PM: see fig. 7).

It is worth noting the difference between peridotite (UL-a) and pyroxenite patterns, except one of the UL-b samples (UL-b3: see Table 1), which shows a very similar pattern to that of the peridotites (fig. 7). Nevertheless, the

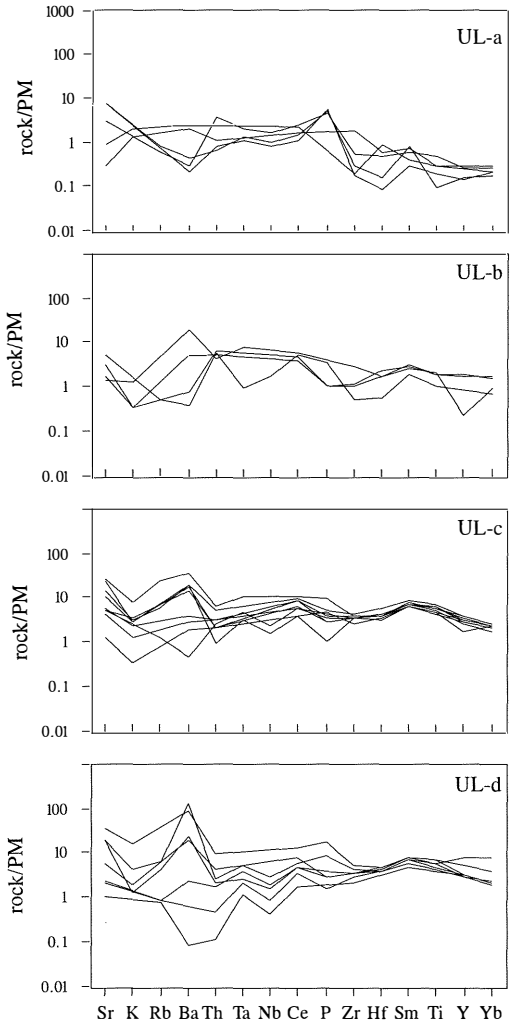

Fig. 7 – PM-normalized multi-element element diagrams of UL xenoliths (normalizing values of Jagoutz *et al.*, 1979, except for Ce and P after Wood *et al.*, 1979a, and Yb after McDonough *et al.*, 1991). Petrographic sub-groups as in fig. 2.

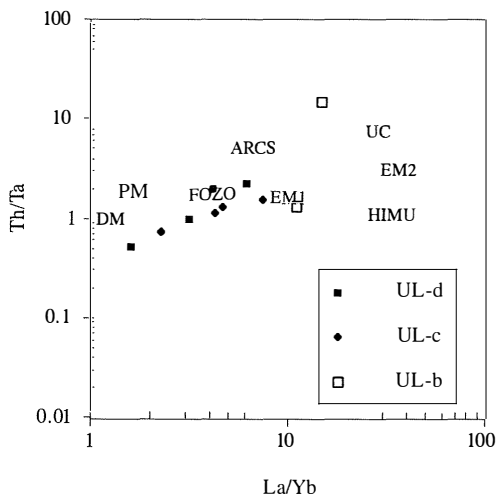

Fig. 8 – La/Yb *vs* Th/Ta binary diagram of some pyroxenite xenoliths. Petrographic sub-groups as in fig. 2. DM: depleted mantle; PM: primordial mantle; FOZO: lower-mantle plume component; UC: upper-continental crust; ARCS: subduction slab related source; HIMU, EM1 and EM2: lower- mantle sources enriched by different contaminating components, as indicated by Tomlison *et al.*, 1999.

distribution of incompatible trace elements in the Iblean ultramafic xenoliths is not a discriminating feature for the proposed groups. The common depletion in HFSE, relatively incompatible elements in our peridotites (UL-a) with respect to PM abundances, is another indication of their residual nature. However, significant enrichment in LILE for both peridotites and pyroxenites reveal the importance of aqueous fluid-driven metasomatic events in the Iblean upper mantle. There is also probably a considerable influence of weathering products (e.g. serpentine, smectites, etc.).

It should also be noted that some bivariate ratios plot Th/Ta *vs* La/Yb (Tomlinson *et al.* 1999) for some UL-c and UL-d pyroxenites with a trend between depleted mantle and FOZO (fig. 8), perhaps indicating the interaction of both components in the petrogenesis of these rocks (e.g. an astenospheric plume intruding a depleted lithosphere).

The distribution of 3d transition metals in our peridotites (UL-a) conforms to PM abundances (fig. 9), except for slight, but variable depletions in Sc, Ti and Cu. This fact confirms the harzburgitic residual character of these rocks, since the distributions of these elements in mantle spinel-peridotites are mostly related to pyroxene and spinel abundances (Vannucci *et al.*, 1991).

UL-b pyroxenites show enrichment in Sc, Ti, V and Cu with respect to PM abundances and a depletion trend from Fe to Ni. Two samples exhibit more evident depletion in Cr and Ni and hence their 3d patterns approach those of diverse primitive MOR basalts (e.g. Rollinson, 1993). This fact endorses the cumulate origin of these two pyroxenites, since pyroxenes, olivine and oxides represent the major mineral phases hosting 3d elements in basalts. The loss of «basaltic» imprinting in the other UL-b samples may be an effect of extensive reactions with the peridotite country rocks at magmatic or sub-solidus temperatures.

Most of the examined UL-c and UL-d pyroxenites show concordant «basaltic» patterns for transition elements, with variable, sometimes significant depletions in Cr (close to 0.01 × PM in some UL-d samples) and Ni (about 0.03 × PM in some UL-d samples) enrichment in Sc, Ti, V and Cu and approximately PM abundances for Mn, Fe and Co (fig. 9). The variable amounts of Cr and Ni depletion with respect to PM abundances may depend on several factors, as well as (1) the nature of the parent primitive liquid: the abundance of these highly compatible elements in primitive melts is closely related to the degree of partial melting of the source, and hence to the alkalinity of the liquid; (2) the variable quantity of intercumulus liquid, poor in transition elements, in the cumulate protoliths; (3) the different evolution grade of the parent melt. Testing the validity of these hypotheses would imply discussion of mineral chemistry data in addition to whole-rock chemistry, which is beyond the scope of the present paper.

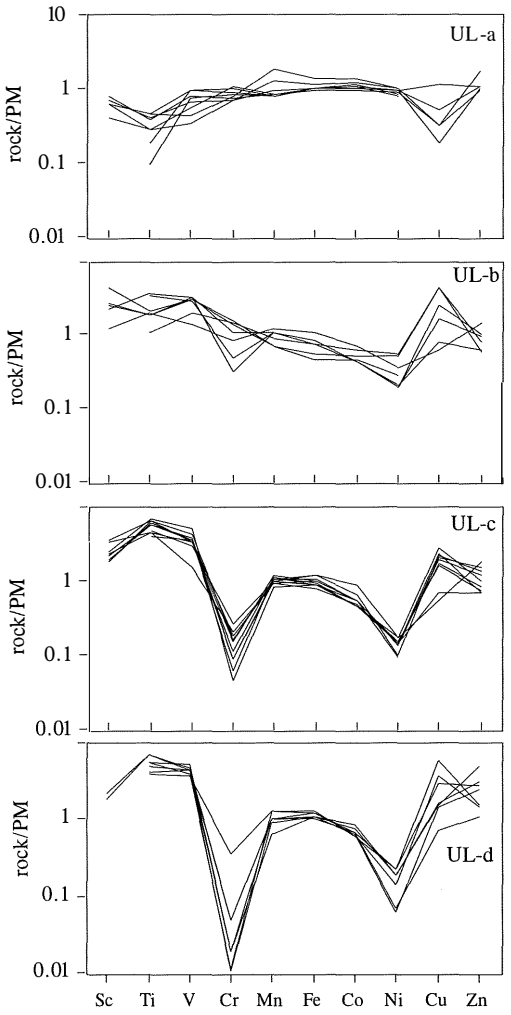

Fig. 9 – PM-normalized transition element variation diagrams for UL xenoliths (normalizing values of Jagoutz *et al.*, 1979). Petrographic sub-groups as in fig. 2.

FELDSPAR-BEARING XENOLITHS

Major elements

The examined FB xenoliths have wide variations in SiO_2 contents (from 38.06 to 59.5%). In more detail, cumulitic gabbros (FB-f) show the largest variations in silica (from 38.6% to 48.44%), whereas mafic granulites (FB-e), anorthosite (FB-g) and websterite (FB-h) are grouped together within a relatively narrow interval (from 50.03 to 51.72% SiO_2). The two dioritic xenoliths show the highest silica contents of all the Iblean xenoliths (56.54 and 59.5%).

Harker binary plots (fig. 10) show that the silica contents of FB-f gabbros are correlated positively with Al_2O_3 and Na_2O and negatively with FeO and TiO_2. These variations suggest that the alumina contents of these rocks depend on plagioclase abundances, whereas iron and titanium distributions are mostly controlled by Fe-Ti oxide accumulation. In fact, the large quantity of the latter minerals can be accounted for by the very low silica contents and elevated TiO_2 and FeO in these rocks, especially in FB-f1 and FB-f3 (see Table 1). There is also a relatively low total content of alkalis compared with silica (e.g. CIPW calculation for sample FB-f1 yields 3.65 mol% of normative nepheline but 11.6 mol% of magnetite and 10.64 mol% of ilmenite).

The two metadiorites (FB-h) exhibit very similar contents of CaO, Na_2O, FeO and MgO but striking differences in TiO_2, P_2O_5 and K_2O (fig. 10). This fact may suggest a common magmatic protolith which underwent different sub-solidus histories. It is also noticeable that these rocks are significantly richer in alkalis than other Iblean xenoliths.

The range of major element variations for the granulites (FB-e) is much narrower than that of the previous groups, except for Al_2O_3. This varies from 14.4% to 24.5%, forming a trend roughly perpendicular to the silica axis, as shown in fig. 10. The alumina content of these rocks therefore depends on both plagioclase and Al-spinel modal abundances. The very low K_2O, P_2O_5 and TiO_2 and the relatively high CaO ratios in these rocks should be noted. Anorthosite (FB-g) and plagioclase-websterite (FB-i) cluster together with the granulites in the Harker plots for P_2O_5, K_2O and TiO_2 (fig. 10), whereas they are distributed at the opposite extremities of the granulite trends in those for Al_2O_3, Na_2O, MgO and FeO (fig. 10). This fact may raise doubts concerning the convenience

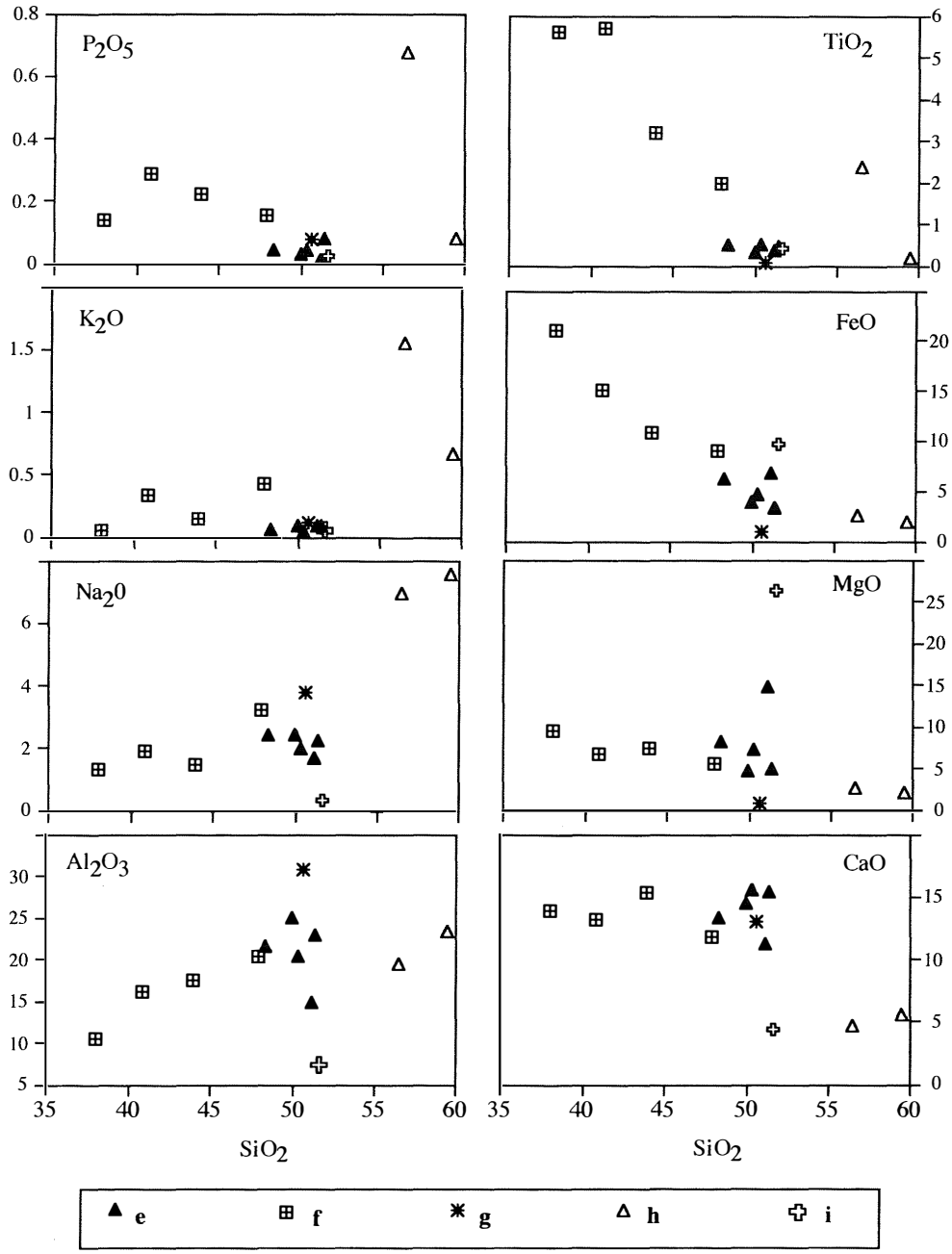

Fig. 10 – Major element variation diagrams for Iblean FB xenoliths as a function of SiO_2. Petrographic sub-groups as in fig. 2.

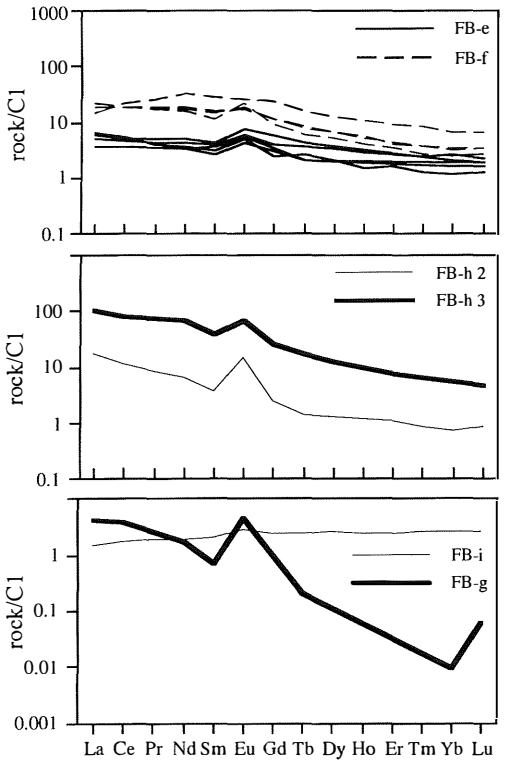

Fig. 11 – C1-normalized REE patterns for FB xenoliths (normalizing values of Boynton, 1984). Petrographic sub-groups as in fig. 2.

of distinguishing both FB-g and FB-i groups from the granulites: nevertheless, we prefer to maintain the proposed divisions because of the striking differences in mineralogic and whole-rock compositions shown by these rock types.

The distribution of our granulites in the bivariate ratio diagram mg* *vs* SiO_2/Al_2O_3 (fig. 4) indicates progressive plagioclase enrichment, starting from the field for primitive basalts. This distribution may confirm the cumulitic nature of the protoliths. Three of the gabbroic cumulates (FB-f) conform to a trend of Fe-oxide accumulation, in agreement with their modal composition. Lastly, note the relatively elevated mg* value (=0.6) of FB-h2 metadiorite despite its low absolute contents of both MgO (=1.85%) and FeO* (=1.45%: see Table 1).

REE distribution

The feldspar-bearing xenoliths belonging to groups FB-e and FB-f have similar C1 normalised REE patterns, with a gentle negative slope and an evident Eu positive anomaly, except for sample FB-f1 (fig. 11), which has a slightly upward-convex pattern. The Eu anomaly conforms to the large quantity of modal feldspar in these rocks, whereas FB-f1 displays a significant accumulation of mafic minerals. Nevertheless, the two groups can

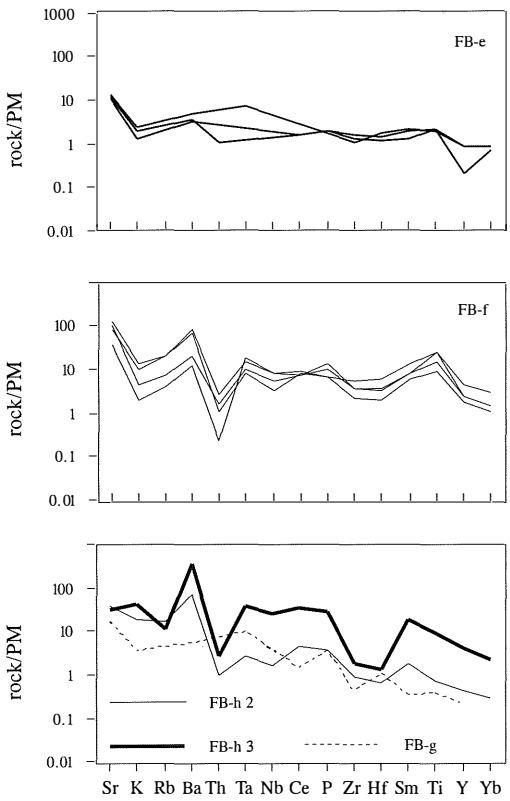

Fig. 12 – PM-normalized multi-element diagrams for FB xenoliths (normalizing values of Jagoutz *et al.*, 1979 except for Ce and P of Wood *et al.*, 1979a and Yb of McDonough *et al.*, 1991). Petrographic sub-groups as in fig. 2

easily be distinguished by their different LREE enrichments (e.g., FB-f shows LREE>10 × C1 with La_n/Sm_n=0.54-1.9 and La_n/Yb_n=2.24-8.84, FB-e<10 × C1 with La_n/Sm_n=0.96-2.12 and La_n/Yb_n=1.81-5.48). This fact may depend on some REE depletion during granulite facies equilibration of presumably magmatic protoliths.

The two metadiorites (LB-h) show quite similar patterns, which differ from the other groups for their steeper slope. But one of the samples (FB-h3) is much richer in REE than the other (FB-h2). The anorthosite REE pattern exhibits an evident positive Eu anomaly and a very steep negative slope (La_n=7 × C1, Yb_n=0.01 × C1) with strong depletion in HREE compared with chondrites. Instead, the plagioclase-websterite (FB-i) exhibits approximate chondritic REE abundances.

Primordial-mantle normalized multi-element diagrams

The gabbroic xenoliths (FB-f) show more elevated contents of incompatible elements, except for Th, than the granulitic group (FB-e) (fig. 12). In particular, the first group shows subparallel, variously indented patterns for LILE and Th, with positive relative anomalies at Sr and Ba (close to 100 × PM) and troughs at Th, with a flat pattern for the HFSE, but evident enrichment in Ti (up to 10 × PM). One sample shows a significant Yb negative anomaly.

The FB-e granulites show gentle negative slopes, from 10 × PM (Sr) to 0.2 × PM (Y) (see fig. 12). As already proposed for REE abundances, LILE depletion in granulites may be a consequence of dehydration during re-equilibration at sub-solidus temperatures.

The two metadiorites (FB-h) have similar incompatible element patterns, with many variations with respect to PM abundances, from about 500 × PM (Ba) to about 1 × PM (Hf). Sample FB-h3 is generally richer in incompatible elements than FB-h2 (fig. 12). Anorthosite (FB-g) shows an incompatible element distribution close to that of granulites (fig. 12). Unfortunately, there is insufficient data for plagioclase-websterite.

The compatible transition element patterns present more or less pronounced negative anomalies in Cr and Ni for all the FB xenoliths examined (fig. 13). This feature may represent imprinting of their primitive basaltic origin and hence the entity of these anomalies may depend on both magmatic and metamorphic differentiation: from Sc to V our magmatic

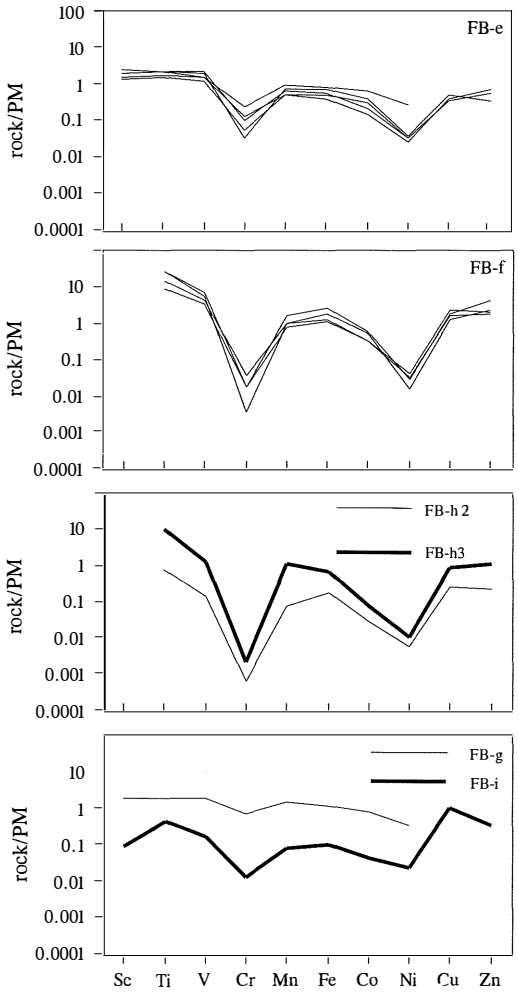

Fig. 13 – PM-normalized transition element variation diagrams for FB xenoliths (normalizing values of Jagoutz *et al.*, 1979). Petrographic sub-groups as in fig. 2.

textured samples show a negative slope, whereas the granulites exhibit a flat pattern at about 1 × PM. The FB-f group also shows enrichment in Cu and Zn.

IBLEAN UPPER-MANTLE AND LOWER-CRUST BULK COMPOSITION INFERRED FROM XENOLITHS

Coupling the percentage volume estimates of the various groups of Iblean xenoliths (fig. 2) with the available data set of chemical analyses, we can calculate the weighted average compositions of the ultramafic and feldspar-bearing xenoliths. The significance of these calculations in terms of reliable bulk compositions of the Iblean upper mantle and inaccessible crust is closely related to the following factors: (1) the grade of representativity of the chemical data with respect to the lithological variety of the Iblean xenoliths; (2) the grade of representativity of the Iblean xenoliths with respect to all parts of the lithospheric column; (3) the congruity of the distribution of xenolith types with respect to the original remote rock masses.

Both mantle and crust compositions (with the above uncertainties) exhibit negative slopes of their C1 normalized REE patterns (fig. 14), except for an evident Eu positive anomaly, which depends on feldspar accumulation in the crust. Also, primordial mantle normalised incompatible element distributions show subparallel trends except for opposite peaks for Ti, which is relatively concentrated in crustal

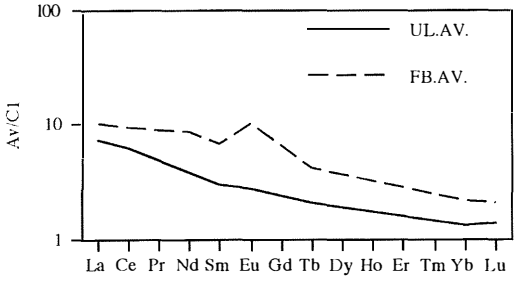

Fig. 14 – C1-normalized REE patterns for averaged UL and FB Iblean xenoliths (normalizing values of Boynton, 1984).

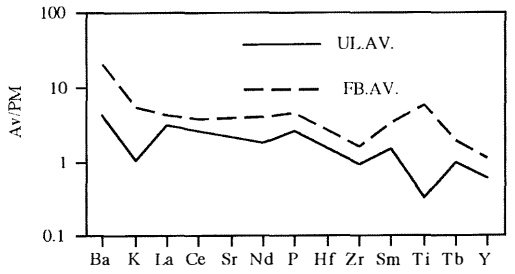

Fig. 15 – PM-normalized multi-element diagrams for averaged UL and FB Iblean xenoliths (normalizing values of Wood *et al.*, 1979a).

mafic minerals (fig. 15). Note the «re-fertilizing» effect of pyroxenite intrusions in refractory peridotites, giving the mantle a bulk composition close to PM. Conversely, PM normalised transition metals show quite different patterns for mantle and crust. The former appear roughly flat at PM abundances, the latter exhibit a pattern close to MORB (Rollinson, 1993), with significant Cr and Ni negative anomalies (fig. 16): it is also evident that bulk crust incompatible and moderately compatible elements closely match MORB abundances, except for Ba (fig. 17: see previous discussion).

CONCLUSIONS

The peridotite xenoliths exhibit a moderately depleted character, with some secondary enrichment due to pervasive or cryptic metasomatism. Pyroxenites represent products

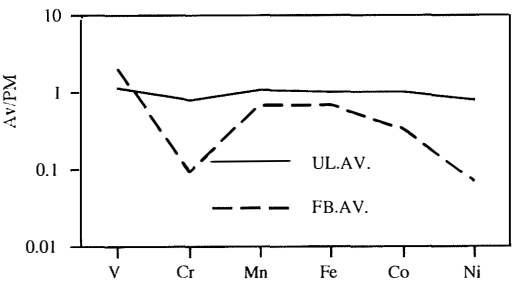

Fig. 16 – PM-normalized transition element variation diagrams for averaged UL and FB Iblean xenoliths (normalizing values of Jagoutz *et al.*, 1979).

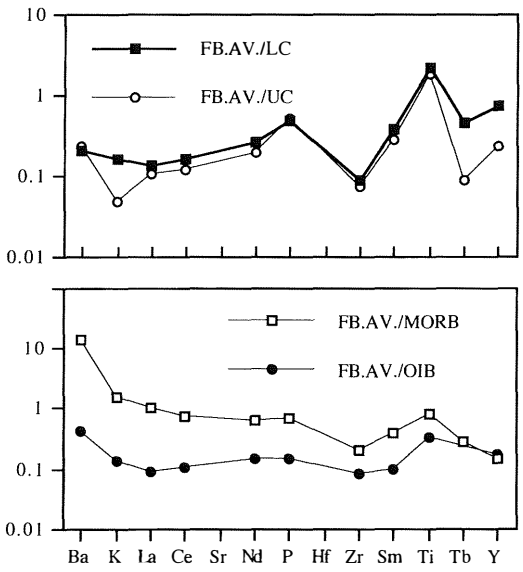

Fig. 17 – PM-normalized multi-element element diagrams for averaged FB Iblean xenoliths (normalizing values of Weaver and Tarney, 1984, Taylor and McLennan, 1981, and Sun, 1980).

of the crystallization of deep-seated magmatic liquids intruding peridotites at different levels of the lithospheric mantle.

The mineralogical, textural and chemical differences between the diverse pyroxenite groups depend on several factors, as well as (1) the nature of the original magmatic liquids (alkaline, tholeiitic, picritic), (2) different fractionation stages of the same liquid, (3) various grades of sub-solidus equilibration, with or without ionic exchange with peridotitic country rocks, etc.

Concerning crustal xenoliths, their more or less distant basaltic parentage is evident. The distribution of some major and trace elements in the calculated bulk Iblean lower crust composition also conform to some basaltic liquids, although there are significant differences in Al_2O_3 and CaO. These may be the effect of some plagioclase accumulation in the crust.

Provided that the Iblean xenoliths represent the lithospheric column quite well, the lack of typical continental upper-crust lithologies (e.g. granites, felsic metaigneous and metasedimentary rocks, etc.) may be attributed to several causes, as well as (1) modification of a previous continental crust by extreme rifting and concomitant magmatic intrusions and underplating, (2) severe erosion of the upper continental crust during an (unknown) period of exhumation, (3) the oceanic nature of the Iblean lithosphere.

A comprehensive discussion of these hypotheses will be given in a further paper on the basis of new petrophysical data (Kern *et al.*, in progress). We note that the last hypothesis (3) is supported by the lack of any contamination by continental crust rocks in the Iblean lavas (Trua *et al.*, 1998). The above-reported abundances and ratios of some trace elements in the Iblean xenoliths also exclude any contamination by crustal materials: for example, the Th/Ta ratios (<1) in some UL and FB xenoliths are far below the lower continental crust ratio (see Tomlinson *et al.* 1999). In addition, the La/Nb ratios (<1.4) of some of our crustal xenoliths may be compatible with an oceanic plateau (Condie, 1999). Some geophysical data, as well as the high magnetic susceptibility of the Iblean inaccessible crust, strong magnetic anomalies, high heat flow density (e.g. Arisi Rota and Fichera, 1987; Bianchi *et al.*, 1987) may also endorse the oceanic affinity of the lithosphere. Instead, some deep seismic refraction data (e.g. crust thickness is estimated about 30 km: Morelli, 1998, and references therein) are compatible with an attenuated continental crust.

ACKNOWLEDGEMENTS

Most of the research was financially supported by CNR – National Group of Volcanology and MURST. Constructive criticism by Profs. F. Innocenti and G. Traversa is gratefully acknowledged. We would like to thank Prof. P. Atzori for useful suggestions.

REFERENCES

ARISI ROTA and FICHERA F. (1987) — *Magnetic interpretation related to geo-magnetic provinces:*

the italian case history. Tectonophysics, **138**, 179-196.

ATZORI P., MAZZOLENI P., PUNTURO R. and SCRIBANO V. (1999) — *Garnet-spinel-pyroxenite xenoliths from Iblean Plateau (South-eastern Sicily, Italy).* Mineral. Petrol., **66**, 215-226.

BECCALUVA L., SIENA F., COLTORTI M., DI GRANDE A., LO GIUDICE A., MACCIOTTA G., TASSINARI R. and VACCARO C. (1998) — *Nephelinitic to tholeiitic magma generation in a transtensional tectonic setting: an integrated model for the Iblean volcanism, Sicily.* J. Petrol., **39**, 1547-1576.

BIANCHI F., CARBONE S., GRASSO M., INVERNIZZI G., LENTINI F., LONGARETTI G., MERLINI S. and MOSTARDINI F. (1987) — *Sicilia orientale: profilo geologico Nebrodi-Iblei.* Mem. Soc. Geol. It., **38**, 429-458.

BOYNTON W.V. (1984) — *Geochemistry of the rare earth elements: meteorite studies.* In: «*Rare earth elements geochemistry*» P. Henderson (ed.), Elsevier, 63-114.

CARBONE S. and LENTINI F. (1981) — *Caratteri deposizionali delle vulcaniti del Miocene superiore negli Iblei (Sicilia sud-orientale).* Geol. Romana, **20**, 79-101.

CONDIE K.C. (1999) — *Mafic crustal xenoliths and the origin in the lower continental crust.* Lithos, **46**, 95-101.

DAWSON J.B. (1980) — *Kimberlites and their xenoliths.* Springer, Berlin Heidelberg New York, 252 pp.

FERRINI V. and SASSANO G. (1999) — *Nature, origin and age of diamonds: a state-of-the-art report.* Per. Mineral., **68**, 109-126.

FREY F.A. (1980) — *The origin of pyroxenites and garnet pyroxenites from Salt Lake Crater, Oahu, Hawaii: trace element evidence.* Am. J. Sci., **280-A**, 427-449.

FREY F.A. and PRINZ M. (1978) — *Ultramafic inclusions from San Carlos, Arizona: petrological and geochemical data bearing on their petrogenesis.* Earth Planet. Sci. Lett., **38**, 129-176.

GRASSO M. (1993) — *Pleistocene structures along the Ionian side of the Hyblean Plateau (SE Sicily): implications for the tectonic evolution of the Malta Escarpment.* In «Geological Development of Sicilian-Tunisian Platform». Proceedings of International Scientific Meeting, University of Urbino, Italy, 4-6 Nov. 1992, 49-54.

HART S.R. and DUNN T. (1993) — *Experimental cpx/melt partitioning of 24 trace elements.* Contrib. Mineral. Petrol., **113**, 1-8.

HAWTHORNE J.B. (1975) — *Model of a kimberlite pipe.* Phys. Chem. Earth, **9**, 1-15.

JAGOUTZ E., PALME H., BADDENHAUSEN H., BLUM K., CENDALES M., DREIBUS G., SPOTTEL B., LORENZ V. and WANKE H. (1979) — *The abundances of major, minor and trace elements in the earth's mantle as derived from primitive ultramafic nodules.* Proc. Lunar. and Planet. Sci. Conf. No 10, Geochim. Cosmochim. Acta, Suppl., **11**, 2031-2050.

KEMPTON P.D., DOWNES H., SHARKOV E.V., VETRIN V.R., IONOV D.A., CARSWELL D.A. and BEARD A. (1995) — *Petrology and geochemistry of xenoliths from the Northern Baltic shield: evidence for partial melting and metasomatism in the lower crust beneath an Archean terrane.* Lithos, **36**, 157-184.

KRETZ R. (1983) — *Symbols for rock-forming minerals.* Am. Min., **68**, 277-279.

LONGARETTI G. and ROCCHI S. (1990) — *Il magmatismo dell'avampaese ibleo (Sicilia Orientale) tra il Trias e il Quaternario: dati stratigrafici e petrologici di sottosuolo.* Mem. Soc. Geol. It., **45**, 911-925.

MAZZOLENI P. and SCRIBANO V. (1994) — *Preliminary geochemical information on selected upper-mantle and lower-crust xenoliths from Hyblean Plateau (South Eastern Sicily).* Miner. Petr. Acta, **37**, 295-305.

MCDONOUGH W.F., SUN S., RINGWOOD A.E., JAGOUTZ E. and HOFMANN A.W. (1991) — *K, Rb and Cs in the earth and moon and the evolution of the earth's mantle.* Geochim. Cosmochim. Acta, Ross Taylor Symposium volume.

MORELLI C. (1998) — *Lithospheric structure and geodynamics of the Italian peninsula derived from geophysical data: a review.* Mem. Soc. Geol. It., **32**, 113-122.

MORTEN L. and OBATA M. (1983) — *Possible high-temperature origin of pyroxenite lenses within garnet peridotite, northern Italy.* Bull. Miner., **106**, 775-780.

NIMIS P. (1998) — *Clinopyroxene geobarometry of pyroxenitic xenoliths from Hyblean Plateau (SE Sicily, Italy).* Eur. J. Mineral., **10**, 521-533.

PUNTURO R. (1997) — *Segnalazione di una lherzolite a flogopite nelle vulcanoclastiti mioceniche della Valle Guffari (Buccheri): evidenza di metasomatismo modale nel mantello sub-ibleo.* Atti Acc. Gioenia Sci. Nat., **31**, 73-87.

PUNTURO R. and SCRIBANO S. (1997) — *Dati geochimici e petrografici su xenoliti di clinopirossenite a grana ultragrossa e websteriti nelle vulcanoclastiti mioceniche dell'alta Valle Guffari (Monti Iblei, Sicilia).* Miner. Petrogr. Acta, **40**, 95-116.

ROLLINSON H.R. (1993) — *Using geochemical data: evaluation, presentation, interpretation.* Longman Group UK Limited, pp. 352.

SCRIBANO V. (1986) — *The harzburgite xenoliths in a Quaternary basanitoid lava near Scordia (Hyblean*

plateau, Sicily). Rend. Soc. It. Mineral. Petrol., **41**, 245-255.

SCRIBANO V. (1987a) — *Origin of websterite nodules from some alkaline volcanic rocks of Hyblean Plateau (South-Eastern Sicily).* Per. Mineral., **56**, 51-69.

SCRIBANO V. (1987b) — *The ultramafic and mafic nodule suite in a tuff-breccia pipe from Cozzo Molino (Hyblean Plateau -SE Sicily).* Rend. Soc. It. Mineral. Petrol., **42,** 203-217.

Scribano V. (1988a) — *Petrological notes on lower-crustal nodules from Hyblean Plateau (Sicily).* Per. Mineral. **57,** 41-52.

SCRIBANO V. (1988b) — *Natural partial melting of pyroxenite nodules and megacrysts from Sicily: a preliminary report.* Per. Mineral. **57**, 65-72

SCRIBANO V. (1995) — *Xenoliti di origine profonda nelle vulcaniti degli Iblei: una finestra aperta sulla litosfera profonda della Sicilia Sud-orientale. Stato delle conoscenze e prospettive future*. In: F. Ferrucci and F. Innocenti (Editors): Progetto-Etna 1993-1995, stato di avanzamento delle ricerche. Giardini, Pisa, 159-164.

SUN S.S. (1980) — *Lead isotopic study of young volcanic rocks from mid-ocean ridges, ocean islands and island arcs.* Phil. Trans. R. Soc., **A297**, 409-445.

TAYLOR S.R. and MCLENNAN S.M. (1981) — *The composition and evolution of the continental crust: rare earth element evidence from sedimentary rocks.* Phil. Trans. R. Soc., **A301**, 381-399.

TOMLINSON K.Y., HUGHES D.J., THURSTON P.C. and HALL R.P. (1999) — *Plume magmatism and crustal growth at 2.9 to 3.0 Ga in the Steep Rock and Lumby Lake area, Western Superior Province.* Lithos, **46**, 103-136.

TONARINI S., D'ORAZIO M., ARMIENTI P., INNOCENTI F. AND SCRIBANO V. (1996) — *Geochemical features of eastern Sicily lithosphere as probed by Iblean xenoliths and lavas.* Eur. J. Mineral., **8**, 1153-1173.

TRUA T., ESPERANÇA S. AND MAZZUOLI R. (1998) — *The evolution of the lithospheric mantle along the N. African Plate: geochemical and isotopical evidence from the tholeiitic and alkaline volcanic rocks of the Hyblean plateau, Italy*. Contrib. Mineral. Petrol., **131**, 307-322.

VANNUCCI, R., SHIMIZU, N., BOTTAZZI P., OTTOLINI, L., PICCARDO G.B. and RAMPONE E. (1991) — *Rare earth and trace elements geochemistry of clinopyroxenes from the Zabargad peridotite-pyroxenite association.* In: Menzies, M.A., Dupuy C. and Nicolas A. (Editors), Orogenic lherzolites and mantle processes, J. Petrol. Spec. Lherzolite Iss., 225-269.

WEAVER B.L. and TARNEY J. (1984) — *Empirical approach to estimating the composition of the continental crust.* Nature, **310**, 575-557.

WOOD D.A., TARNEY J., VARET J., SAUNDERS A.D., BAUGAULT H., JORON J.L., TREUIL M. and CANN J.R. (1979a) — *Geochemistry of basalts drilled in the North Atlantic by IPOD Leg 49: implications for mantle heterogeneity*. Earth Planet. Sci. Lett., **42**, 77-97.